Vision Res. Vol. 14, pp. 1421-1432. Pergamon **Press** 1974. Printed in Great Britain.

THE SIMULTANEOUS SPATIAL FREQUENCY SHIFT: A DISSOCIATION BETWEEN THE DETECTION AND PERCEPTION OF GRATINGS

S. KLEIN,[1] C. F. STROMEYER III and L. GANZ

Department of Psychology, Stanford University, Stanford, California 94305, U.S.A.

(Received 4 September 1973; *in revised form* 19 *April* 1974)

Abstract—Previous studies have shown that adaptation to a *sinusoidal grating* raises the contrast threshold for detecting gratings of similar spatial frequency and causes a shift in the apparent frequency of gratings of neighboring spatial frequency. In the present study the *threshold rise* and *frequency shift* were studied under two conditions: after adapting to a grating *(successive* condition) and while the test grating was surrounded by an inducing grating *(simultaneous* condition). The frequency shift was quantitatively similar under both conditions. Furthermore, the simultaneous shift was found to have the same dependence on the inducing contrast and orientation as did the successive shift. A rise in the threshold of the test grating, however, was found only in the successive condition. This indicates that the threshold rise and frequency shift are dissociated. A one-stage neural model was examined to see whether the frequency shift could be quantitatively predicted from the threshold rise. The predictions were poor. A two-stage model was thus proposed to account for the results.

INTRODUCTION

Prolonged viewing of a high-contrast grating may produce two striking aftereffects. First, the contrast required to detect a grating of similar orientation and spatial frequency may be elevated (Pantle and Sekuler, 1968; Blakemore and Campbell, 1969; Graham, 1972). This threshold elevation effect (Blakemore and Campbell, 1969) is frequency-selective, with a 1 octave bandwidth: the threshold is maximally elevated for sinusoidal gratings at the adapting spatial frequency, and the elevation effect falls to half strength for test gratings about 1/2 octave either side of the adapting frequency. Stromeyer and Julesz (1972) showed that the same tuning function describes the threshold visibility of vertical sinusoidal gratings which were masked by superposed vertical noise stripes of limited bandwidth. The noise acts as an adapting grating in selectively raising the threshold of the test grating. These studies provide evidence for the existence of spatial frequency tuned channels in the human visual system.

Blakemore and Sutton (1969) observed a second striking aftereffect produced by adaptation to a high contrast grating. Test gratings of somewhat lower frequency than the adapting grating appeared even lower after adaptation; conversely, higher frequency test gratings appeared even higher. The frequency shift can also be demonstrated with random texture and print (Walker, 1966; Mayhew, 1973; Anstis, 1973). [It is interesting to note that there is a similar frequency shift in hearing (von Bekesy, 1929). Adaptation to a loud tone both reduces the loudness of tones near the adapting frequency and causes the pitch of tones of neighboring frequency to appear shifted further away from the adapting frequency.]

Blakemore and Sutton (1969) proposed a simple explanation for the visual frequency shift. The brain is said to perceive the frequency of a grating by identifying the frequency-selective neural element that responds maximally or by identifying some other measure of central tendency of the response distribution. Adaptation to a grating depresses the sensitivity of those elements that respond to the adapting grating. After adaptation, a grating of neighboring frequency will produce a response distribution whose peak or other measure of central tendency is skewed away from the adapting frequency where sensitivity has been maximally depressed, and thus the apparent frequency of the test grating will appear shifted away from the adapting frequency.

According to this explanation the apparent frequency shift can be quantitatively predicted from the threshold elevation function, because the frequency shift and threshold elevation are simply two different manifestations of a common state of neural adaptation. This is called a one-stage model of spatial frequency processing. Two tests of this model are described in the present paper. In Part I experimental observations are presented comparing frequency shifts generated by simultaneous and successive induction. The frequency shift, as measured under the two conditions, was quantitatively similar: when the test grating was presented simultaneously with a surround grating of the same orientation (simultaneous induction), and when the test grating was viewed after adapting to a full-field grating (successive induction). However, a

[1] Present address: Joint Science Department, Claremont Colleges, Claremont, California 91711, U.S.A.

threshold elevation effect occurred only after adapting to the full-field grating (successive) and did not occur when the test grating was surrounded by an inducing grating (simultaneous). Thus, the two effects—frequency shifts and threshold elevations—can be dissociated, which suggests that the one-stage model is incorrect. In Part II a theoretical analysis of the successive induction of the spatial frequency shift is presented. A one-stage model is described explicitly. It is shown how the frequency shift can be predicted from the threshold elevation function. When the predicted frequency shifts are compared to experimental results, significant discrepancies are found both in magnitude and distribution. This further suggests that the one-stage model is incorrect. A possible two-stage model which could encompass the results is described in the Discussion.

METHODS

Figure 1 shows the stimulus configuration used to study the simultaneous apparent frequency shift. (Square-wave gratings are shown in the figure, but sinusoidal gratings were used in the experiments.) In the simultaneous condition, two sinusoidal gratings were in a concentric, contiguous disk-annulus configuration: the inducing grating in the annulus surrounded the test grating in the disk. In the successive condition, a sinusoidal adapting grating that filled the entire annular and disk area was presented prior to the small, concentric test disk. Positioned below these patterns was a horizontal grating, which could be adjusted to match the apparent spatial frequency of the vertical test pattern in the disk.

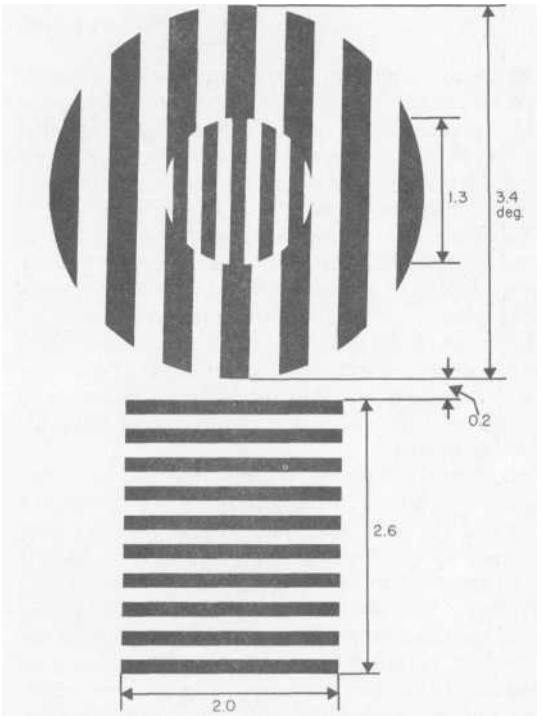

Fig. 1. The stimuli used to study the simultaneous spatial frequency shift. The inducing grating in the annulus surrounds the test grating in the center disk. The subject adjusts the horizontal grating to match the apparent frequency of the test grating. (Sinusoidal gratings were used in the experiments, although square-wave gratings are shown here.)

Two ground glass rear-projection screens were positioned at right angles. Each screen was 157 cm away from the subject's eye. The screens were optically combined by a beam splitter cube placed just before one of the subject's eyes. A photographic transparency of the sinusoidal inducing grating was projected on one screen, and the test grating was projected on the other screen. The screens had opaque masks fixed to their surfaces to obtain the desired geometric configurations. A lens near the eye was used to reduce the retinal size of the display by a factor of 1/3 (producing the angular sizes specified in Fig. 1); a second lens placed the display at optical infinity. A 4 mm artificial pupil and chin rest helped keep the stimuli aligned on the retina.

The adjustable, horizontal grating was generated on an oscilloscope tube following the method of Campbell and Green (1965). The subject could vary the spatial frequency of this grating by turning the frequency knob on the sine-wave generator. One complete turn of the knob changed the frequency by 6 per cent. Spatial frequency was read with a digital frequency meter.

The photographic transparencies of sinusoidal gratings were made from the oscilloscope and processed in two steps (negative-positive) for a product gamma of 1·0. The final positives were measured on a microdensitometer to assure that the gratings had low harmonic distortion (for details see Stromeyer, Lange and Ganz, 1973). A Fourier analysis of the microdensitometer traces indicated that the *total* harmonic distortion was 4-5 per cent. The projected transparencies were equated with filters to the chromaticity and mean spatial luminance (7·6 cd/m^2) of the white phosphor, P-4, of the oscilloscope. Mean spatial luminance measured through the optics was 1·6 cd/m^2; retinal illuminance, 20 td.

The inducing and test gratings were typically oriented vertically; the comparison field grating, however, was horizontal, so that it would not be influenced by an orientation-specific, apparent frequency shift produced by the inducing or test grating. To study the orientation-selectivity of the frequency shift, the inducing grating in the annulus was tilted away from vertical with a Dove prism. The spatial frequency of the test grating was always maintained at 3·8 c/deg; the frequency of the inducing grating differed from the test grating in 1/4 octave steps or multiples thereof.

The contrast of the film gratings was approximately 60 per cent, although the contrast of the three finest gratings was slightly less. The contrast of the grating on the oscilloscope was adjusted so that it appeared to match the contrast of the test grating. In some experiments the contrast of the inducing grating in the annulus was varied by mixing the grating beam with a homogeneous beam via polarizers (see Campbell and Green, 1965). Mean luminance and chromaticity were kept constant by using color correcting filters.

PART I. RESULTS: EXPERIMENTAL

Spatial frequency shift

Demonstration of the simultaneous frequency shift. The reader may see for himself the simultaneous fre-

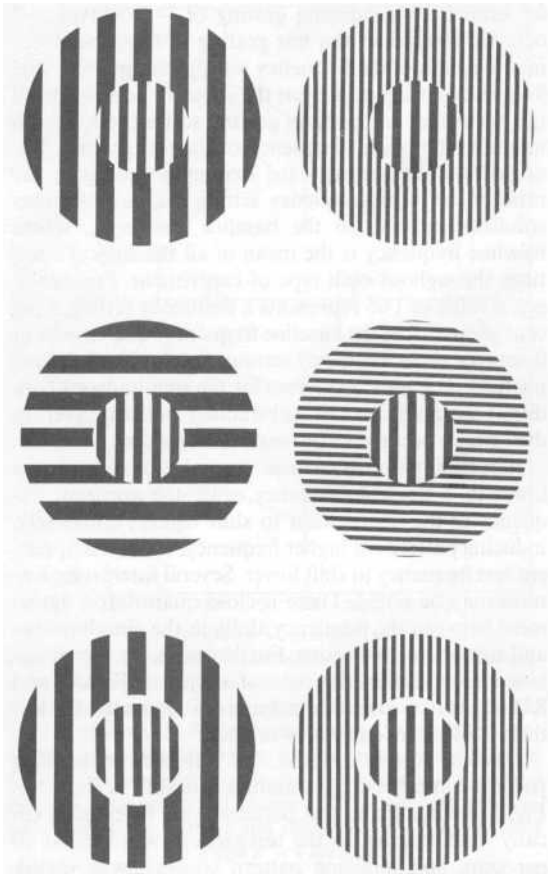

Fig. 2. Demonstration of simultaneous frequency shift. In the upper section, two small vertical test gratings of identical spatial frequency are surrounded by gratings of different spatial frequencies. The test gratings, however, appear to have different spatial frequencies: the test grating with the lower frequency surround appears to have a higher frequency than the grating with the higher frequency surround. In the middle section, the surround gratings are horizontal. The apparent frequency shift largely disappears, which shows that the frequency shift is orientation-selective. In the bottom section, the frequency shift may be seen although the surround inducing grating and center test grating are separated by small rings. Thus, the process causing the frequency shift can propagate over small distances.

quency shift in Fig. 2. Square-wave gratings are depicted, due to the difficulty in reproducing sinusoidal gratings. In the upper section, two small vertical test gratings of identical spatial frequency are surrounded by gratings of different spatial frequencies. The test gratings, however, do not appear to be of identical frequency: the grating with the lower frequency surround appears to have a higher frequency than the grating with the higher frequency surround. In the middle section, the reader can see that this illusion largely disappears when the inducing gratings are oriented horizontally with respect to the test gratings, thus demonstrating that the frequency shift is orientation-specific. The bottom section shows that the frequency shift occurs even when a small ring separates the inducing and test gratings. Thus, the process producing the frequency shift can propagate over small distances. MacKay (1973) also shows several versions of the simultaneous shift, including an analog to the Craik-O'Brien-Cornsweet illusion of brightness. A demonstration of the successive shift may be found in Blakemore, Nachmias and Sutton (1970).

Measuring the frequency shift. The frequency shift was measured under conditions of simultaneous and successive induction. The subjects were the three authors and one naive subject.

The subject first dark adapted several minutes. For the simultaneous condition the stimulus sequence was: 2-sec warning tone during which the subject fixates a dim fixation light; 1-sec flash of disk-annulus centered on fixation light; 3-sec period to look down and adjust the spatial frequency of the horizontal grating in the comparison field so that it matches the apparent frequency of the test grating (see Fig. 1). The comparison field was constantly visible; the disk-annulus was dark except during the 1-sec flash. The subject repeatedly viewed this sequence until he was satisfied with his match and then the experimenter offset the frequency adjustment knob for the next match. The spatial frequency of the test grating was always 3·8 c/deg. The frequency of the inducing grating was set for each match either higher or lower than the test frequency, spanning a range 2 octaves either side of the test frequency in 1/4-octave steps (or sometimes 1/2-octave steps). A blank annular surround was also used; its luminance matched the mean luminance of the gratings. In a single session all inducing frequencies were used just once, and typically eight sessions were run on each subject. In some experiments, either the contrast or the orientation of the inducing grating in the annulus was varied.

In the successive induction condition, the subject initially adapted 2 min to a vertical grating that covered the entire area of disk and annulus (see Fig. 1). Thereafter, every 11 sec the adapting pattern was replaced by a 1-sec presentation of the vertical test grating in the disk area. After each presentation of the test grating, the subject quickly adjusted the frequency of the horizontal comparison grating to match the apparent frequency of the test grating and then continued adapting. The subject stated when he was satisfied with his match. A number of matches were collected before moving on to the next adapting frequency. A rest of 20-30 min intervened between each adapting frequency.

Each panel of Figs. 3 and 4 shows the simultaneous frequency shifts (filled circles) and successive frequency shifts (open circles) for each subject. The abscissa represents the spatial frequency of the inducing gratings in both cycles/deg and octaves relative to the test frequency. The test frequency was maintained at 3·8 c/deg, which is designated 0 octaves on the octave abscissa scale and which is indicated by an arrow. Thus,

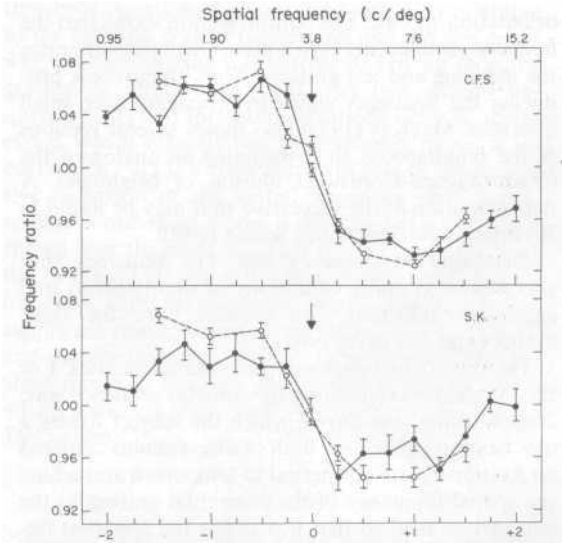

Fig. 3. The effect of inducing gratings on judgements of apparent spatial frequency. Each panel shows results for Subjects CFS and SK plotted separately. The spatial frequency of the inducing grating is shown on the top abscissa scale; the bottom scale shows inducing frequency in octaves relative to the test frequency. The test frequency at 0 octaves is indicated by an arrow. Symbols are the geometric means with S.E. *(n* = 8) of the frequency settings. Open circles are mean settings for the successive condition and filled circles are the mean settings for the simultaneous condition. The symbol x shows mean settings for a blank inducing field. For inducing gratings below the test spatial frequency, the test grating appeared higher in frequency on the average; conversely, for inducing frequencies higher than the test frequency, the test grating appeared lower.

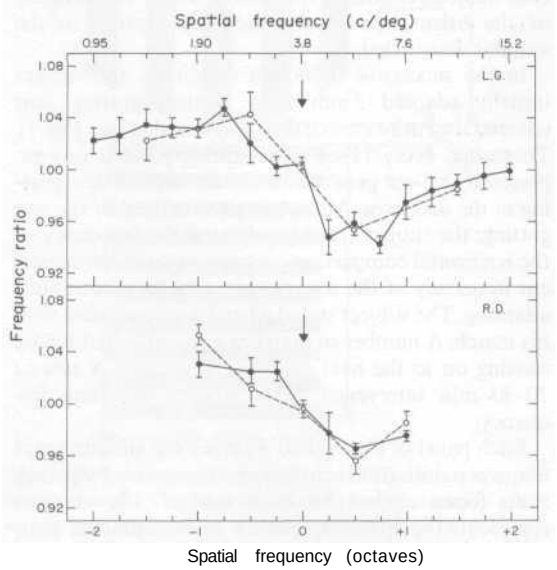

Fig. 4. Same legend as Fig. 3. Results for Subjects LG and RD (for Subject RD, *n* = 8; for LG, *n* = *6* for simultaneous shift and *n* = 4 for successive shift).

for example, an inducing grating of -2 octaves is 2 octaves lower than the test grating at 0 octave. Geometric means of the frequency settings are plotted. The frequency settings represent the subject's adjustment of the horizontal comparison grating so that it appeared to match the spatial frequency of the test grating. The ordinate scale expresses the frequency setting as the ratio of the mean frequency setting for each stimulus condition relative to the baseline frequency, where baseline frequency is the mean of all the subject's settings throughout each type of experiment. For example, a value of 1·05 represents a frequency setting 5 per cent greater than the baseline frequency. The crosses at 0 octaves show frequency settings for the blank inducing field. The standard errors for the simultaneous condition were reduced by subtracting out any average drift which occurred from session to session.

Inducing patterns whose spatial frequencies are lower than the test frequency cause the apparent frequency of the test pattern to shift higher; conversely, inducing patterns of higher frequency, cause the apparent test frequency to shift lower. Several interesting features may be noted. There is close quantitative agreement between the frequency shifts in the simultaneous and successive conditions. Furthermore, for the simultaneous condition, the data of subjects SK, LG and RD (the naive subject) are typically separated by less than 1 S.E. from subject to subject.

Inducing pattern contrast. The influence of inducing pattern contrast on the simultaneous shift is shown in Fig. 5. Inducing and test patterns were oriented vertically. The contrast of the test pattern was held at 60 per cent, and inducing pattern contrast was varied. Each curve represents the magnitude of the shift for a single spatial frequency of the inducing surround. The shift clearly falls off as the contrast of the inducing pattern is reduced.

Orientation-selectivity. Figure 6 shows that the simultaneous shift is orientation-selective. All gratings

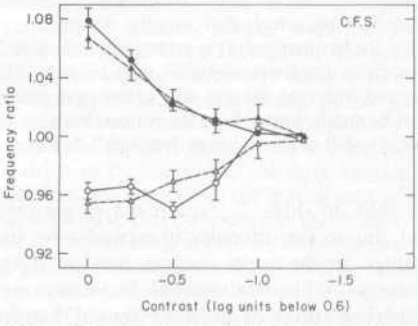

Fig. 5. The effect of contrast of the inducing grating on the simultaneous spatial frequency shift. Both inducing and test gratings were vertical. The test grating contrast was 0·6; the contrast of the inducing grating was varied as shown on the abscissa. Each curve is for a different spatial frequency of the inducing grating, measured relative to the test frequency at 3·8 c/deg: −1 octave ●; −1/2 octave ▲; +1/2 octave △; +1 octave ○. The symbols are geometric means of settings and their S.E. (*n* = 7, for Subject CFS).

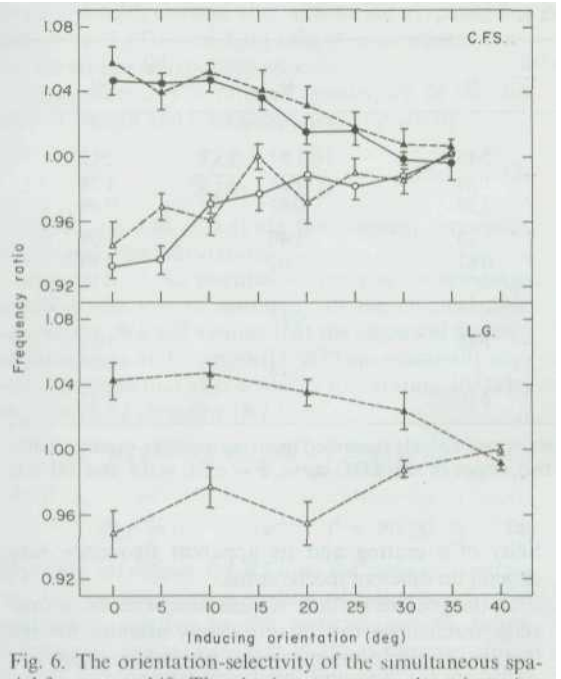

Fig. 6. The orientation-selectivity of the simultaneous spatial frequency shift. The abscissa represents the orientation of the inducing grating in deg clockwise from the vertical test orientation, *viz.* 0 deg. Each curve is for a different spatial frequency of the inducing grating, measured relative to the test frequency at 3·8 c/deg: −1 octave ●; −1/2 octave ▲; +1/2 octave △; +1 octave ○. The symbols are geometric means of settings and their S.E. ($n = 6$ for Subject CFS and $n = 4$ for LG).

were maintained at 60 per cent contrast. The magni tude of the frequency shift decreased as the inducing grating was tilled clockwise away from the vertical orientation of (the test grating. Much curve is for a different spatial frequency of the inducing grating. In each session, one match was made for every stimulus condition, and the data points are means combining several sessions.

Blakemore and Nachmias (1971) determined the orientation-selectivity of the successive frequency shift by an "equivalent contrast" transformation. Tilting the inducing grating away from the test orientation reduces the shift; alternatively, not tilting the inducing grating but reducing its contrast reduces the shift. Blakemore and Nachmias found that the frequency shift could be reduced an equivalent amount either by decreasing the adapting contrast by 50 per cent or by maintaining the contrast at its original value and tilting the adapting grating 6 3/4° away from the test orientation. The threshold elevation phenomenon behaved similarly. Kulikowski (1972) has found an average value of 71/4° for the threshold elevation measured on four subjects. The same equivalent contrast transformation on the data for the simultaneous shift (for Subject CFS) yields a value of 71/4°. In other words, the function that relates strength of spatial frequency shift to the orientation of the inducing grating is highly similar in the simultaneous and successive conditions.

Threshold elevation phenomenon

Blakemore *et al.* (1970) and Blakemore and Nachmias (1971) argue that the two aftereffects produced by prolonged adaptation to a grating the threshold elevation and the spatial frequency shift are caused by modifying the sensitivity of a single set of neural mechanisms that underlies both effects. The present experiment examines whether the threshold elevation and frequency shift can be dissociated. A dissociation would suggest that the two effects depend on different mechanisms. The previous experiment showed that a very similar frequency shift was produced by simultaneous and successive induction. Will these two modes of stimulation produce equivalent threshold elevations?

I he test pattern was displayed on the oscilloscope. The oscilloscope was masked down to a circular held that exactly filled the hole in the annular inducing Held (sec Fig. 1). Thresholds were measured under two conditions: (I) successive condition the full-field inducing grating was presented prior to the test pattern; (2) simultaneous condition the inducing surround (annulus) and test grating (center disk) were presented simultaneously. The test grating was always horizontal. and the inducing patterns were vertical or horizontal. (The *vertical orientation* was a control condition. It will be remembered that the spatial frequency *shift* is ***orientation-selective.***) All gratings were 3·8 c/deg. Inducing gratings were 60 per cent contrast; the test grating could be varied in 1/40-log contrast steps with a step attenuator.

It soon appeared that the threshold elevation was very small or non-existent in the simultaneous condition, and to more definitely measure any weak effect, a signal detection technique was adopted (Green and Swets. 1966).

A run consisted of 100 trials in which the test pattern was either a blank or a horizontal grating of constant contrast throughout the run. The test patterns were chosen using a random number table. Blanks and grat ings occurred with equal probability.

In the successive condition, the subject initially adapted 2 min to the full-field horizontal adapting grating or to the vertical control grilling, and every 11 sec thereafter the adapting pattern was replaced by a 1-sec presentation of the test pattern a horizontal grating or a blank field. While observing the adapting grating, the subject moved his eyes about continuously to prevent forming an after-image of the grating.

For the simultaneous condition. The subject fixated on a tiny point in the center of the oscilloscope field. Every 11 sec the annular surround grating was presented for 1 see, during which the test pattern on the oscilloscope came on for the first 0·3 sec of the l-sec surround presentation. The annular field was dark except during the l-sec presentation, whereas the test field was always maintained at a constant mean

Table 1.

Subject	Contrast, test grating (%)	$\sigma_n/\sigma_s = 0{\cdot}8$		$\sigma_n/\sigma_s = 1{\cdot}0$	
		H	*V*	*H*	*V*
Simultaneous presentation					
C.F.S.	2·26	2·20	2·45	1·87	2·12
	1·80	1·45	1·50	1·36	1·28
	1·43	0·75	0·57	0·67	0·49
S.K.	3·20	1·57	1·20	1·40	1·09
	2·54	1·15	0·82	1·02	0·80
Successive presentation					
C.F.S.	2·54	0·95		0·83	
	1·26		1·55		1·31
S.K.	2·54	1·01		0·89	
	1·43		2·16		1·92

Detectability, d', of horizontal test grating with simultaneously or successively presented inducing gratings, oriented either horizontally, *H*, or vertically, *V*. Values of d' are shown for two slopes of the ROC curve. $\alpha = \sigma_n/\sigma_s = 0{\cdot}8$ and 1·0. S.E. of $d' < 0{\cdot}3$.

luminance. The test pattern was either a horizontal grating or a blank field and was preceded by a 2-sec warning tone. Every 10 trials of the 100-trial run the surround inducing grating was switched from a vertical to a horizontal orientation.

For every test trial the subject gave a confidence rating on a whole number scale, 1-5, where 1 means definitely a blank and 5 means definitely a grating. The ratings were used to plot ROC curves (Egan, Schulman and Greenberg, 1959). The data were plotted on double probability paper, and a straight line was fitted to the data by the method of least squares. The value of d' was read from the horizontal intercept. Each value of d' was based on approximately 100 observation trials.

The results in Table 1 show values of d' for each of two values of the slope of the ROC curves—$\alpha = \sigma_n/\sigma_s = 0{\cdot}8$ and 1·0. The conclusions hold for both values of a. The standard error for each value of d' is approximately ±0·3. (Appendix 1 gives reasons for using ROC curves of specific slope and shows the variance calculations.)

For the *simultaneous* condition, the threshold of the horizontal grating is equally affected by the vertical and horizontal surround gratings. In contrast, adapting to the horizontal grating in the *successive* condition raises the threshold contrast of the horizontal test grating by a factor of two or more above the threshold measured after adapting to the vertical grating. This can be seen from Table 1 where the detectability of the successively presented horizontal grating is sharply reduced even though its contrast is approximately doubled.

PART II. RESULTS: THEORETICAL

Theoretical analysis of one-stage model

Thus far it has been shown that the apparent spatial frequency shift behaves very similarly under both simultaneous and successive induction. However, the threshold elevation phenomenon was observed only under successive induction. This suggests that the visibility of a grating and its apparent frequency may depend on different mechanisms.

In the present section, we examine whether a one-stage mechanism can quantitatively account for the frequency shift in the successive case where there is a threshold elevation. The simplest explanation of the frequency shift states that the apparent frequency of a grating depends upon the distribution of responses of broadly tuned spatial frequency channels (Blakemore and Sutton, 1969). Thus, adapting to a grating will skew the response distribution away from the adaptation frequency. Two versions of the one-stage model will be examined. One version assumes that the perceived frequency of a grating is determined by the peak of the skewed response distribution; the second version assumes that the apparent frequency is determined by the product moment of the skewed response distribution. Several assumptions are made in order to predict the apparent frequency shift from a distribution of neural responses.

Assumption 1. An assumption is made to clarify the notion of "channel". A channel is thought of as a group of neurones with a selective response to particular test patterns. The response of a channel is given by the product of two factors: a factor which depends upon the test pattern and a factor independent of the test pattern which specifies the sensitivity of the channel. The channel sensitivity can be changed by adaptation. The adaptation of a channel can be expressed in the following mathematical form.

The response of a channel to a particular test pattern after adaptation is equal to the response of that channel prior to adaptation multiplied by the reduced sensitivity caused by adaptation:

$$R_J(T,A) = R_J(T,0) \cdot S_J(A)/S_J(0) \qquad (1)$$

where $R_J(T,A)$ represents the response of the *J*th channel to a test pattern of spatial frequency *T*, after adaptation at spatial frequency *A*, and $S_J(A)$ is the sensi-

tivity of the *J*th channel after adaptation at spatial frequency *A*. $R_J(T,0)$ and $S_J(0)$ refer to preadaptation response and sensitivity respectively.

Assumption 2. The ratio of sensitivities of the Jth channel before and after adaptation is given by

$$\frac{S_J(A)}{S_J(0)} = \frac{c_{th}(0)}{c_{th}(A)} \tag{2}$$

where c_{th} (0) and c_{th} *(A)* are the contrast thresholds before and after adaptation.

Assumption 3. An essential property of the one-stage model is the loss of sensitivity of the channel after adaptation. We will assume that the empirical findings of Blakemore and Campbell (1969) are essentially correct. They find that after adapting to a grating, the relative threshold elevation *(RTE)* is

$$RTE = (c_{th}(A)/c_{th}(0)) - 1 = \Phi(f_J/f_A) \tag{3}$$

where

$$\Phi(f) = (e^{-kf^2} - e^{-4kf^2})^2 \times F(c_A). \tag{4}$$

Equation (3) defines the *RTE* as the ratio of contrast needed for detecting a grating of frequency f_J after adaptation relative to the contrast needed before adaptation, minus one—that is, the percentage elevation of the contrast threshold. Equation (4) says that the adapting contrast C_A does not change the shape of the *RTE* function, as was shown experimentally by Blakemore and Campbell (1969). The term $F(c_A)$ in equation (4) specifies how the magnitude of the threshold elevation depends upon adapting contrast. The constant *k* is given the value 0462 so that the function peaks at $f = 1$ (that is, where $f_A = f_J$).

Combining equations (1-3) gives

$$R_J(T,A) = R_J(T,0)/[1 + \Phi(f_J/f_A)]. \tag{5}$$

Assumption 4. It is assumed that

$$R_J(T,0) \propto \Phi(f_J/f_T). \tag{6}$$

The response of the Jth channel before adaptation is assumed to be proportional to the relative threshold elevation function of Blakemore and Campbell (1969).

Assumption 5. An assumption must now be made about how the response function $R_J(T,A)$ gets mapped onto perceived frequency. Two models for perceived frequency will be considered. (1) The *product moment model* in which the perceived frequency is the average frequency, weighted by the response function $R_f(T,A)$. The percent frequency shift A is given by

$$\Delta = \frac{\int f_J R_J(T,A)\,df_J}{f_T \int R_J(T,A)\,df_J} - \frac{\int f_J R_J(T,0)\,df_J}{f_T \int R_J(T,0)\,df_J}. \tag{7}$$

(2) The *peak response model* assumes that the perceived frequency corresponds to the channel which responds maximally. The maximally responding channel can be found by setting the derivative of $R_J(T,A)$ with respect to// equal to zero.

$$\frac{dR_J(T,A)}{df_J} = 0. \tag{8}$$

For this model the percent frequency shift A = $(f_J - f_T)/f_T$ where f_J is the peak of the response distribution after adaptation, obtained from equation (8), and f_T/ is the peak of the response distribution before adaptation. Equations (7) and (8) were solved with a digital computer.

How well does the model predict the frequency shift? Figure 7 shows data of the present experiment, taken from Figs. 3 and 4. Filled circles indicate the simultaneous frequency shift and open circles indicate the successive shift. Each point is a geometric mean combining data of CFS, SK and LG. The abscissa represents inducing frequency relative to test frequency; test frequency is 3·8 c/deg, designated zero octave. The dashed curve is the prediction from the peak response model, and the solid curve is the prediction from the product moment model. For these calculations, the peak of the *RTE* function was normalized to 1·5 (the adapted threshold was approximately 2·5 times the unadapted threshold).

Figure 8 shows data on the successive shift taken from Fig. 3 of Blakemore *et al.* (1970). They adapted to gratings from 2·5 to 14·2 c/deg, at 1/2-octave steps. Test gratings spanned an interval about 2 octaves either side of the adapting frequency. Circles are geometric means combining all their data. Data are transformed so that the abscissa represents the adapting frequency relative to the test frequency—at zero octave. For example, the point at +2 octaves represents all

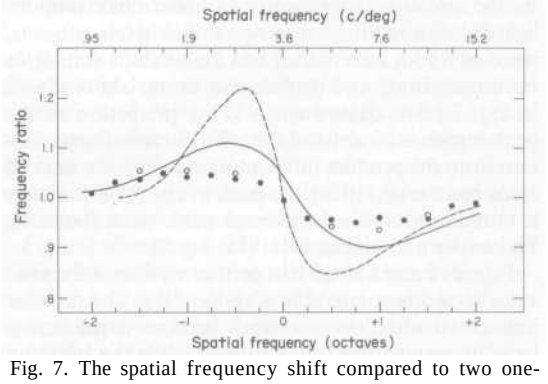

Fig. 7. The spatial frequency shift compared to two one-stage models. The data points are geometric means of the frequency shifts for Subjects CFS, SK and LG combined, taken from Figs. 3 and 4, where filled circles indicate the simultaneous shift and open circles indicate the successive shift. The abscissa represents the spatial frequency of the inducing grating relative to the test frequency—designated 0 octaves. The dashed curve is the prediction from the peak response model (the perceived frequency is determined by the maximally responding channel); the solid curve is the prediction from the product moment model (the perceived frequency is given by the weighted mean of the channel responses). The relative threshold elevation factor needed for predicting the magnitude of the frequency shift was taken to be 1·5, which was the value found in the present experiment with successive induction. Note that both models predict shifts which are too large. The product moment model predicts a shift even when adapting and test frequencies are identical.

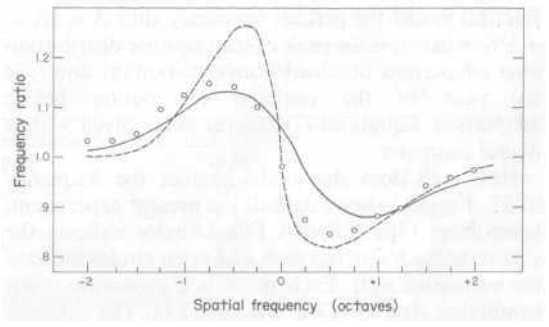

Fig. 8. The spatial frequency shift found by Blakemore *et al.* (1970) is compared to two theoretical models. The axes and curves are similar to Fig. 7 except that the relative threshold elevation factor needed for the predictions was taken to be 2·0 instead of 1·5. This factor was obtained from Blakemore and Nachmias (1971, Fig. 7). The frequency shift data is gotten by averaging the successive shifts in Fig. 3 of Blakemore *et al.* (1970), where the average is taken over all test frequencies for both their subjects combined.

cases for which the adapting frequency was 2 octaves above the test frequency. Blakemore *et al.* express the frequency shift in terms of the period ratio; however, Fig. 8 shows the frequency as the frequency ratio, which is simply the reciprocal of the period ratio. Note that their shifts are considerably larger than the shifts in the present experiments. [J. Nachmias (unpublished) measured the successive shift with six subjects, three of whom were naive, and found shifts similar in both magnitude and distribution to our shifts shown in Fig. 7.] The dashed curve is the prediction of the peak response model and the solid curve is the prediction from the product moment model. For the data of Blakemore *et al.* (1970), the peak of the *RTE* function is normalized to 2—the average peak value found by Blakemore and Nachmias (1971, Fig. 7).

Figures 7 and 8 show that neither version of the one-stage model is compatible with the data. The product moment model does not work because it predicts a large frequency shift (> 5 per cent) when the adapting frequency is the same as the test frequency. In addition, for adapting frequencies between the test frequency and 1/4-3/4 octave above the test frequency, the perceived spatial frequency shift of Blakemore *et al.* is significantly greater than the product moment prediction. On the other hand the peak response model disagrees with the data most severely for adapting frequencies below the test frequency. The predicted frequency shifts are too large for $f_A > 1/2 f_T$, and are too small for $f_A < 1/3 f_T$. A general statement can be made about the shape of the predicted frequency shift: since the threshold elevation curve is asymmetric around the inducing frequency, the predicted shift will also be asymmetric. However, the actual shifts in Figs. 7 and 8 are fairly symmetric. In Appendix 2, two of the assumptions of the peak response model are relaxed and the same conclusions are still obtained.

DISCUSSION

A one-stage model of spatial frequency perception hypothesizes that a sinusoidal grating activates a number of tuned spatial frequency channels, and the spatial frequency that is actually perceived results from a mechanism of central tendency, for example, one which selects the channel most excited. Adaptation introduces a proportionate bias which skews or shifts perception away from the most adapted region. Three flaws have been found in this model. First, the spatial frequency shift is strikingly similar in magnitude and distribution when induced either simultaneously or successively. This similarity suggests that both induction procedures are affecting the same mechanism, thus attenuating its potency in some way. However, a rise in the detection threshold is only found with successive induction. This means that the spatial frequency shift can be dissociated from the threshold elevation phenomenon. Secondly, the one-stage model predicts a specific magnitude of frequency shift from a given amount of successive adaptation. But the observed shift was considerably smaller than predicted from the peak model. Thirdly, the one-stage peak model predicts a sharp fall-off in the frequency shift for a test frequency of more than 1 octave above the adapting frequency; i.e. for an adapting frequency of more than 1 octave below the test frequency in Figs. 7 and 8. The observed shifts do not show this fall-off. The product moment model, on the other hand, predicts a frequency shift when adapting and test frequencies are identical. However, there is no evidence for such a shift.

All three results suggest that the spatial frequency shift and threshold elevation effect may occur at different levels of the nervous system. The effects may require a two-stage model. A possible model is now presented.

An image on retinal Area A is processed by a variety *of analyzers* tuned to various orientations and spatial frequencies. Each analyzer has a receptive field with, say, an on-center and off-surround. The analyzers feed into a *detection* pooling mechanism, and presumably the subject detects a grating when analyzers reach threshold level. The analyzers also have a second output onto *integrators*. The integrators have a broader spatial frequency response than the analyzers, for each integrator has inputs from a range of analyzers. Some measure of central tendency of the response distribution of the integrators is extracted, and this gives rise to the *perception* of spatial frequency.

In the successive induction paradigm, the subject inspects an adapting grating for a duration sufficient to strongly fatigue those analyzers sensitive to the adapting frequency and to more weakly fatigue analyzers tuned to adjacent frequencies. Fatigue also occurs at the integrator stage. The spread of fatigue covers a broader range of spatial frequencies at the integrator level than at the analyzer level, because each integrator has inputs from a range of analyzers.

After fatigue has been induced, the contrast required

to detect a grating presented on the same retinal area will rise (Blakemore and Campbell, 1969). The distribution of the threshold elevation phenomenon reflects the spread function of the analyzers, or their spatial frequency tuning characteristic.

In a task involving spatial frequency matching or identification of the period of the grating, the subject uses the central tendency of the distribution of integrator activity. Fatigue in the integrators will introduce a systematic bias in this measure of central tendency, and this may give rise to a shift in apparent spatial frequency.

In the simultaneous induction paradigm, the test and surround gratings are presented simultaneously —the test pattern to retinal Area A and the surround to Area B. *Integrators* with similar spatial frequency tuning and orientation tuning characteristics are joined from Area A to Area B by inhibitory connections. Thus integrators of similar tuning characteristics inhibit each other. As a result, the reduction in potency of the integrators representing Area A resembles the distribution of fatigue effects in the integrators representing Area B. Thus the bias effects in the integrators are similarly distributed in the two cases of simultaneous and successive induction, and the spatial frequency shifts are also highly similar, which is what we observed. Likewise, only integrators with similar orientation tuning inhibit each other. Thus the orientation-selectivity is similar for simultaneous and successive frequency shifts.

The analyzers, used for detecting a grating, are not joined by inhibitory connections from Area A to Area B—unlike the integrators. Thus in the simultaneous induction conditions, the analyzers representing Area A are not fatigued or inhibited by the surround grating in Area B. Thus, no threshold rise will occur when a test grating is presented to Area A. The fatigued integrator network is simply not used for detection tasks according to this model. The analyzers are used to detect gratings, whereas the integrators give rise to the perception of spatial frequency.

Our analysis leads us to conclude, therefore, that (1) the neurophysiological mechanisms underlying visual judgments are organized hierarchically (two levels at the very least), and (2) in different sorts of visual tasks, the subject is capable of tapping information at different levels. This conclusion receives further support from a recent study in which it was shown that the effective harmonic component of a masking stimulus changes when the nature of the visual judgment changes (Carpenter and Ganz, 1972).

The model depicted in this paper, while based entirely on data from psychophysical experiments is compatible with neurophysiological analysis of the visual system. The principle of hierarchical organization has been involved explicitly in the concepts of simple, complex and hyper-complex receptive fields in visual cortex (Hubel and Wiesel, 1959, 1962, 1965), and also in the retinal analysis of motion (Barlow and Levick, 1965). Our finding that visual judgments of spatial frequency involves interpretation of information from mechanisms of similar orientations but somewhat diverse spatial frequencies is compatible with the functional cytoarchitecture of the visual system in which neurones of similar orientations but somewhat diverse receptive field dimensions are collected together in columns of the visual cortex (Hubel and Wiesel, 1962). Another postulated principle is that mechanisms of similar tuning characteristics inhibit each other. There is no neurophysiological evidence for this in the spatial frequency domain, but it appears to operate between color receptors in the retina (Alpern and Rushton, 1965) and at the cortex in the orientation domain (Blakemore and Tobin, 1972).

We have concluded that perceptual judgments of spatial frequency occur at a different level in the visual system than do simple detection judgments. This has been deduced from an experimental and theoretical dissociation of the two types of tasks. It is interesting, therefore, to note that comparable dissociations occur with other visual aftereffects. Consider first tilt-aftereffects. Adaptation to a grating raises the threshold visibility of gratings of the same spatial frequency (detection judgment) and also causes a test grating to appear tilted away from the adapting orientation (Gilinsky and Mayo, 1971). However, Parker (1972) has shown that the tilt-effect is equally strong, when after adapting to a 5 c/deg grating, the test grating frequency is either 5 c/deg or 1 octave higher or lower than 5 c/deg. But the threshold visibility of gratings one octave away from the adapting frequency is little affected by adaptation (Blakemore and Campbell, 1969). Thus the tilt effect and grating visibility may be dissociated. Shattuck and Held (1974) however, observed that color-contingent tilt-effects are somewhat frequency-selective. And Georgeson (1973) observed frequency-selectivity for a simultaneous tilt effect, produced with gratings in a disk-annulus display, similar to Fig. 1.

Figural aftereffects may also require a multi-stage model. Adaptation to a square figure causes displacement of a test line placed near the contour of the square; however, large displacements occur where the threshold visibility function would predict none (Ganz, 1964; Ganz and Day, 1965).

Acknowledgements—This study was supported by grant NSF GB1592 to Stanford University. We wish to thank Dr. Arthur Lange for assistance with equipment and Mrs. Cecilia Bahlman for help with the manuscript. C. F. Stromeyer III thanks Karl Pribram for his continued support.

REFERENCES

Alpern M. and Rushton W. A. H. (1965) The specificity of the cone interaction in the after-flash effect. *J. Physiol., Land.* 176, 473-482.

Anstis S. M. (1973) Size adaptation to visual texture and print: Evidence for spatial frequency analysis. *Am. J. Psychol.* (In press).

Barlow H. B. and Levick W. R. (1965) The mechanism of directionally selective units in rabbit's retina. *J. Physiol., Lond.* 178, 477-504.

Bekesy, G. von (1929) Zur Theorie des Horens; Uber die Bestimmung des einem reinem Tonempfinden entsprechenden Erregungsgebietes der Basilarmembran vermittelst Ermudungserscheinungen. *Physik. Zeits.* 30, 115-125. Reprinted in English in *Experiments in Hearing,* (edited by Wever E. G.), pp. 354-368. McGraw-Hill, New York.

Blakemore C. and Campbell F. W. (1969) On the existence of neurones in the human visual system selectively sensitive to the orientation and size of retinal images. *J. Physiol., Loud.* 203, 237-260.

Blakemore C. and Nachmias J. (1971) The orientation specificity of two visual after-effects. *J. Physiol., Lond.* 213, 157-174.

Blakemore C., Nachmias J. and Sutton P. (1970) The perceived spatial frequency shift: evidence for frequency-selective neurones in the human brain. *J. Phvsioi., Lond.* 210, 727-750.

Blakemore C. and Sutton P. (1969) Size adaptation: A new after-effect. *Science, N.Y.* 166, 245-247.

Blakemore C. and Tobin E. A. (1972) Lateral inhibition between orientation detectors in the cat's visual cortex. *Expl Brain Res.* 15,439-440.

Campbell F. W. and Green D. G. (1965) Optical and retinal factors affecting visual resolution. *J. Phvsioi., Lond.* 181, 576-593.

Carpenter P. A. and Ganz L. (1972) An attentional mechanism in the analysis of spatial frequency *Percept. Psychophys.* 12, 57-60.

Egan J. P., Schulman A. I. and Greenberg G. Z. (1959) Operating characteristics determined by binary decisions and by ratings. *J. acoust. Soc. Am.* 31, 768-773.

Ganz L. (1964) Lateral inhibition and location of visual contours: An analysis of figural after-effects. *Vision Res.* 4, 465-481.

Ganz L. and Day R. H. (1965) An analysis of the satiation-adaptation mechanism of figural after-effects. *Am. J. Psvchol.* 78, 345-361.

Georgeson M. A. (1973) Spatial frequency selectivity of a visual tilt illusion. *Nature, Lond.* 245, 43-45.

Gilinsky A. S. and Mayo T. H. (1971) Inhibitory effects of orientational adaptation. *J. opt. Soc. Am.* 61, 1710-1714.

Gourevitch V. and Galanter E. (1967) A significance test for one parameter isosensitivity functions. *Psychometrika* 32, 25-33.

Graham N. (1972) Spatial frequency channels in the human visual system: Effects of luminance and pattern drift rate. *Vision Res.* 12, 53-68.

Green D. M. and Swets J. A. (1966) *Signal Detection Theory and Psyehophysics.* John Wiley, New York.

Hubel *D.* H. and Wiesel T. N. (1959) Receptive field of single neurones in the cat's striate cortex. *J. Physiol., Lond.* 148, 574-591.

Hubel D. H. and Wiesel T. N. (1962) Receptive fields, binocular interaction and functional architecture in the cat's visual cortex. *J. Physiol, Lond.* 160, 106-154.

Hubel D. H. and Wiesel T. N. (1965) Receptive field and functional architecture in two non-striate visual areas (18 and 19) of the cat. *J. Neurophysiol.* 28, 229-289.

Kulikowski J. J. (1972) Orientational selectivity of human binocular and monocular vision revealed by simultaneous and successive masking. *J. Physiol., Lond.* 226, 67-68 P.

MacKay D. M. (1973) Lateral interaction between neural channels sensitive to texture density? *Nature, Lond.* 245, 159-161.

Mayhew J. E. W. (1973) Movement aftereffects contingent on size: Evidence for movement detectors sensitive to direction of contrast. *Vision Res.* 13, 1789-1795.

Nachmias J. and Kocher E. (1970) Detection and discrimination of luminance increments. *J. opt. Soc. Am.* **60,** 382-390.

Pantle A. and Sekuler R. (1968) Size-detecting mechanisms in human vision. *Science, N.Y.* 162, 1146-1148.

Parker D. M. (1972) Contrast and size variables and the tilt aftereffect. *Q. Jl exp. Psychol.* 24, 1-7.

Shattuck S. and Held R. (1974) Color-contingent tilt aftereffect interacts with spatial frequency and also produces stereo depth. Paper presented to meeting of Eastern Psychological Association, April, 1974.

Stromeyer C. F. III, Lange A. F. and Ganz L. (1973) Spatial frequency phase effects in human vision. *Vision Res.* 13, 2345-2360.

Stromeyer C. F. III and Julesz B. (1972) Spatial-frequency masking in vision: Critical bands and spread of masking. *J. opt. Soc. Am.* 62, 1221-1232.

Walker J. T. (1966) Textural aftereffects: Tactual and visual. Doctoral dissertation. University of Colorado.

APPENDIX 1

Variance in the signal detection experiment

The ROC curves for detection of a grating were fit by a least squares technique. This technique provides a good estimation for d' as long as sparsely populated rating categories are given appropriately small weights. The least squares technique, however, underestimates the standard error of d' since it does not take into account the correlation between the z scores of neighboring rating categories. In this appendix, an *overestimate* of the standard error of d' shall be calculated by assuming there is only one significant criterion level.

The distribution of hits, P_s, is expected to be slightly wider than the distribution of false alarms, P_n (Green and Swets, 1966; Nachmias and Kocher, 1970). Therefore the slope of the ROC curves, $a = -\sigma_n/\sigma_s = 1/\sigma_s$ was chosen to have a value of either 1·0 or 0·8. The results in Table 1 hold for both values. Since these values of a should bracket the actual value, the conclusions reached about the threshold elevation should be valid for the actual value of a.

The derivation of the standard error of d' given by Gourevitch and Galanter (1967) must be slightly modified since a need not equal 1. The ROC curve can be expressed by normal deviates:

$$z_s = \alpha(z_n - d').$$

Thus,

$$d' = z_n - z_s/\alpha.$$

The variance is given by $\text{var } d' = \text{var } z_n + 1/\alpha^2 \text{ var } z_s$. Since

$$P = \frac{1}{\sqrt{2\pi}} \int_{-\infty}^{z} e^{-x^2/2}\, dx$$

and

$$\frac{dP}{dz} = \frac{1}{\sqrt{2\pi}} e^{-z^2/2}$$

then

$$\text{var } z = 2\pi e^{z^2} \text{ var } P = 2\pi e^{z^2} P(1-P)/N$$

since $\text{var } P = P(1-P)/N$ for Poisson statistics, where N is the total number of observations. For P between 0·15 and

0·83 as is the case for most of our data, the function e^z P(1 - P) lies within 0·25 and 0·35. N for our data ranges between 40 and 60. Thus

$$\begin{aligned}\text{var } d' &= 2\pi e^{z_n^2} P_n(1 - P_n)/N_n \\ &\quad + 2\pi/\alpha^2\, e^{z_s^2} P_s(1 - P_s)/N_s \\ &\simeq 2\pi(1 + 1/\alpha^2)0{\cdot}30/50 \simeq 0{\cdot}08.\end{aligned}$$

There were usually two criterion levels for each run which had P_s and P_n between 0·15 and 0·85. Thus the average d' has a variance somewhat less than an individual variance, and the standard error is

$$\begin{aligned}\text{S.E. } d' &= \sqrt{(\text{var } d')} \\ &< 0{\cdot}3.\end{aligned}$$

APPENDIX 2

The theoretical argument against a one-stage model of the frequency shift can be strengthened by relaxing two of the assumptions of the peak response model. The *shape* of the frequency shift function can still be predicted. Assumption 4, $[R_J(T,0) \propto \Phi(f/f_T)]$, which may have been the weakest of the assumptions can be eliminated. Assumption 2 can be modified as follows:

$$\frac{S_J(A)}{S_J(0)} = \left[\frac{c_{th}(0)}{c_{th}(A)}\right]^k \tag{9}$$

where k is allowed to be different from 1.

Combining equations (1, 3, 8 and 9) gives

$$\frac{dR_J(T,0)}{df_J}\Big/R_J(T,0) = \frac{k\, d\Phi(f_J/f_A)}{df_J}\Big/[1 + \Phi(f_J/f_A)]. \tag{10}$$

To evaluate the left hand side of equation (10) we can make a Taylor's series expansion of $R_J(T,0)$ in powers of the percent frequency shift $A = (f_J - f_T)/f_T$. If the frequency shift is small the non-leading terms can be neglected and the derivative term is proportional to A. To first order in A the frequency shift is thus given by

$$\Delta \propto \frac{d\Phi(f_J/f_A)}{df_J}\Big/[1 + \Phi(f_J/f_A)]. \tag{11}$$

This result gives a zero parameter fit to the shape (but not magnitude) of the frequency shift since the function $\Phi(f)$ is determined from the threshold elevation measurements. Inspection of Figs. 7 and 8 show that the peak response prediction disagrees with the actual shifts even after an arbitrary magnitude adjustment is made.

Résumé—Les etudes antérieures montrent que l'adaptation a un reseau sinusoidal augmente le seuil de contraste pour détecter des reseaux de frequence spatiale semblable et produit un decalage dans la frequence apparente des reseaux de frequence spatiale voisine. Dans la presente etude, on étudie l'élévation du seuil et le decalage de frequence dans deux conditions: apres adaptation a un reseau (condition successive) et pendant que le reseau test est entouré par un reseau inducteur (condition simultanée). Le decalage de frequence est quantitativement semblable dans ces deux conditions. En outre le decalage simultané depend du contraste inducteur et de son orientation comme le decalage successif. Au contraire on ne constate d'élévation du seuil du reseau test que dans la condition successive. Ceci indique une dissociation entre elevation du seuil et decalage de frequence. On examine sur un modele nerveux a un étage si on peut prédire quantitativement le decalage de frequence a partir de l'élévation du seuil. Les predictions sont médiocres. On propose donc un modele a deux niveaux pour rendre compte des résultats.

Zusammenfassung—Nach früheren Untersuchungen wird durch Adaptation auf ein Sinusgitter die Kontrastschwelle für Gitter mit ähnlicher Ortsfrequenz angehoben und ihre scheinbare Ortsfrequenz verschoben. Diese Schwellenänderung und Ortsfrequenzverschiebung werden in der vorliegenden Arbeit unter zwei Bedingungen untersucht; nach Adaptation auf ein Gitter (sukzessiv) und in Gegenwart eines das Testgitter umgebenden induzierenden Gitters (simultan). Die Frequenzverschiebung war unter beiden Bedingungen quantitativ ähnlich und hing bei simultaner Darbietung ähnlich von Kontrast und Orientierung des Induktionsgitters ab wie bei sukzessiver Darbietung. Ein Schwellenanstieg zeigte sich jedoch nur bei sukzessiver Darbietung. Dies zeigt, dass Schwellenänderung und Frequenzverschiebung voneinander unabhängig sind. Es wurde untersucht, ob mit einem einstufigen neuralem Modell sich die Frequenzverschiebung aus der Schwellenänderung quantitativ ableiten lässt. Die Vorhersagen waren schlecht. Um die Ergebnisse erklären zu können, wird ein zweistufiges Modell vorgeschlagen.